

Analyzing of Coordinate Operational of UPFC based on Matrix Converter and Wind Turbine Generator under Unbalanced Load

Murtaza Farsadi¹, Farzad Mohammadzadeh Shahir², Darioush Nazarpour¹, and Farhad Nazari Heris³

¹Faculty of Electrical and Computer Engineering, University of Urmia, Urmia, Iran

m_farsadi@yahoo.com, d.nazarpour@urmia.ac.ir

²Department of Electrical Engineering, Khosroshahr Branch, Islamic Azad University, Khosroshahr, Iran

f.m.shahir@gmail.com

³Department of Electrical Engineering, Heris Branch, Islamic Azad University, Heris, Iran

nazari.h.f@gmail.com

Nomenclature

$Index\ i$	Index to show input side quantities
$Index\ o$	Index to show output side quantities
$m_b\ b = i, o$	Modulation index of b side
$\delta_b\ b = i, o$	Phase angle of b side
$\omega_b\ b = i, o$	Switching angular frequency of b side
$\phi_b\ b = i, o$	Phase difference of b side
I_i	Peak value of input current
V_o	Peak value of output voltage
$I_{i,k}\ k = a, b, c$	Input current of phase k in b side
$V_{o,k}\ k = a, b, c$	Output voltage of phase k in b side
I_i^*	Reference of input current vector
V_o^*	Reference of output voltage vector
T_s	Switching time in a period
$T_\kappa, T_\gamma, T_\alpha, T_\beta$	Switching times in adjacent vectors
$d_\kappa, d_\gamma, d_\alpha, d_\beta$	Duty cycles in adjacent vectors
$d_{b,0}\ b = i, o$	Zero duty cycle in b side
$T_{b,0}\ b = i, o$	Zero switching time in b side

Abstract

The flexible ac transmission systems (FACTS) were installed on power systems in order to improve performance of power system such as voltages, active power flows, reactive power flows, and etc. One of the these devices is unified power flow controller based on matrix converter (UPFC-MC) that space vector modulation (SVM) technique can be used switching pattern of its nine-bidirectional switches. In the other hand, distributed generation (DG) systems, such as wind turbine generator farm (WTGF), were installed on power system to provide needed demand energy. This paper presents two coordinate operating schemes for UPFC-MC and WTGF under unbalanced loads. By applying UPFC-MC and WTGF under two proposed controlling methods improve transmission lines power flows were increased. The validity of proposed schemes is reconfirmed by simulation results with MATLAB/Simulink software.

1. Introduction

Flexibility controlling of a power system can be achieved by FACTS devices and many researchers tried to introduce more solutions for suitable using of them for increasing security, capacity and reducing losses of power grids [1-2]. One of the FACTS devices is unified power flow controller (UPFC) that can be controlled different parameters of power network simultaneously that was introduce by Gyughi in 1991 firstly [3]. Various structure and different controlling schemes have been presented for UPFC. One of the best presented structures is based on matrix converter [4-5]. The matrix converter structure is consisting of nine-bidirectional switches with high frequencies switching that directly transmit the energy in ac/ac mode applying no electrolyte capacitor. High operation speed, high qualitative input and output currents, adjustable power factor, and lower size, in addition to possessing no electrolyte capacitor in dc link are important advantage of matrix converter topologies. However, it has some disadvantage such as restricting voltage transfer ratio up to 0.86 and requiring numerous high power semiconductor devices capable of high frequency switching. But, according to its advantages and comparing with other FACTS devices, it can be said that it is a quick ac/dc/ac converter. On other hand, DG system are introduced for provide needed demand and quickly response of power system to load variations that is installed the nearest to load [6]. One of the DG systems is WTG that many researches have been presented in order to analyze its impacts on power flow improving [7, 8], increasing reliability [9], improving stability [10] and etc. In some research, the WTG were considered a WTGF in order to achieve higher power [11]. The UPFC-MC structure has been presented in [4-5] and its controlling scheme are presented in [12] and [13] for balanced and unbalanced loads, respectively. Also, the dynamic model and stability evaluation of UPFC-MC has been described in [14-15] to optimum control in power system and attenuate rotor oscillations of synchronous generator. In this paper, a coordinate operating of UPFC-MC and WTGF with two proposed strategies is analyzed. For this aim, a UPFC-MC structure and its switches controlling strategies, and WTGF are introduced firstly. So, the two proposed schemes for coordinating control are presented. Finally, the impacts of UPFC-MC and WTGF are evaluated on power flows with MATLAB/Simulink under unbalanced loads that are changing dynamically.

2. UPFC-MC

2.1. Structure of UPFC-MC

The UPFC topology is shown in Fig. 1. As it can be seen, the UPFC has nine-bidirectional switches, and input and output passive filters that connected to power system with $Y-Y$ type transformer in shunt side and $\Delta-\Delta$ type transformer in series side. The input and output passive filters are used to eliminate high frequency component of input three-phase currents and output three-phase voltages. The input three-phase currents

relation of UPFC-MC in shunt side is presented as follows [13,16-17]:

$$\begin{aligned} I_{i,a} &= I_i \cos(\omega_i t - \phi_i) \\ I_{i,b} &= I_i \cos(\omega_i t - \phi_i - 120^\circ) \\ I_{i,c} &= I_i \cos(\omega_i t - \phi_i - 240^\circ) \end{aligned} \quad (1)$$

The output three-phase voltages relation of UPFC-MC in series side is defined as follows [13, 16-17]:

$$\begin{aligned} V_{o,a} &= V_o \cos(\omega_o t - \phi_o) \\ V_{o,b} &= V_o \cos(\omega_o t - \phi_o - 120^\circ) \\ V_{o,c} &= V_o \cos(\omega_o t - \phi_o - 240^\circ) \end{aligned} \quad (2)$$

2.2. Modulation Technique

As it mentioned in Fig. 1, the UPFC-MC has nine bidirectional switches that each one of them has two states (on or off). So, there are $2^9 = 512$ possible switching modes, but 27 switching modes are permitted during each switching modes which is due to impossibility of short circuit input three phases and open circuit output three phases. The Venturini [18] and SVM [19] switching technique were presented for controlling 27 known switching modes of UPFC-MC.

The currents of three input phases in shunt side and the voltages of three output phases in series side makes base of SVM controlling method. The rectifiers operating of UPFC-MC provided by shunt side and the inverter operating of UPFC-MC can be controlled by series side. The rectifiers operating controlled by the input current space vector hexagon which is shown in Fig. 2(a) and the inverter operating controlled by the output voltage space vector hexagon that is shown in Fig. 2(b).

Two adjacent vectors (I_x and I_k), and a zero vector ($I_{i,0}$) indicate the reference input current vector on each six section of the input current space vector hexagon as follows [19]:

$$I_i^* = \frac{T_\kappa}{T_s} I_\kappa + \frac{T_\gamma}{T_s} I_\gamma + \frac{T_{i,0}}{T_s} I_{i,0} = d_\kappa I_\kappa + d_\gamma I_\gamma + d_{i,0} I_{i,0} \quad (3)$$

In above relation, d_κ , d_γ , and $d_{i,0}$ parameters were defined as follows[19]:

$$d_\kappa = m_i \sin(60^\circ - \delta_i) \quad (4)$$

$$d_\gamma = m_i \sin(\delta_i) \quad (5)$$

$$d_{i,0} = 1 - d_\kappa - d_\gamma \quad (6)$$

Replacing (4) to (6) into (3), the duty cycle and modulation index of related section extracted as follows, respectively [19]:

$$d_{i,1} = d_\kappa + d_\gamma = m_i \sin(60^\circ - \delta_i) + m_i \sin(\delta_i) \quad (7)$$

$$m_i = \frac{i_i \sqrt{3}}{i_{dc}} \quad (8)$$

Also, two adjacent vectors (V_α and V_β), and a zero voltage vector ($V_{o,0}$) indicates the reference output voltage vector on each six section of the output voltage space vector hexagon as follows [19]:

$$V_o^* = \frac{T_\alpha}{T_s} V_\alpha + \frac{T_\beta}{T_s} V_\beta + \frac{T_{o,0}}{T_s} V_{o,0} = d_\alpha V_\alpha + d_\beta V_\beta + d_{o,0} V_{o,0} \quad (9)$$

In above relation, d_α , d_β , and $d_{o,0}$ parameters were defined as follows [19]:

$$d_\alpha = m_o \sin(60^\circ - \delta_o) \quad (10)$$

$$d_\beta = m_o \sin(\delta_o) \quad (11)$$

$$d_{o,0} = 1 - d_\alpha - d_\beta \quad (12)$$

Replacing (10) to (12) into (9), the duty cycle and modulation index of related section defined as [19]:

$$d_{o,1} = d_\alpha + d_\beta = m_o \sin(60^\circ - \delta_o) + m_o \sin(\delta_o) \quad (13)$$

$$m_o = \frac{v_o \sqrt{3}}{v_{DC}} \quad (14)$$

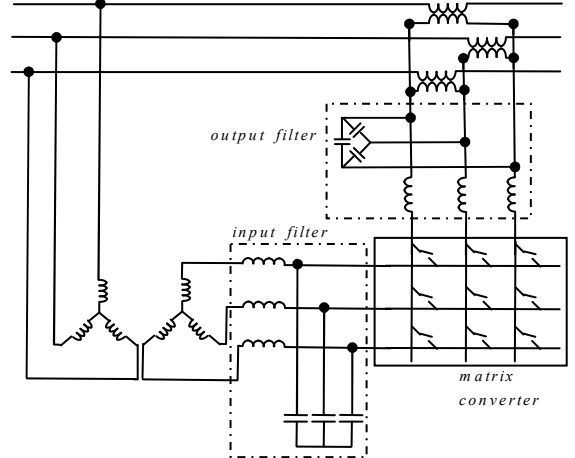


Fig. 1. Structure of UPFC-MC

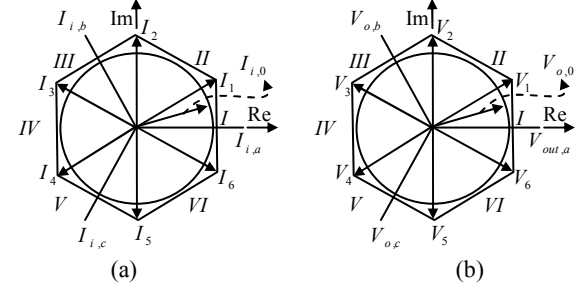


Fig. 2. SVM technique; (a) input current; (b) output voltage

3. Wind Turbine Generator Farm

Distributed generation systems were installed in the nearest place to loads in order to provide needed demand powers. One of these systems is wind turbine generator (WTG). The WTG provide variable power for each wind speed that is shown in Fig. 3. The more numbers of WTG can be installing to near together to achieve more powers that is called WTGF. The output power of a wind turbine generator is calculated as follows [6-11]:

$$P_{WTG} = \begin{cases} 0 & v < v_{cri} \\ P(A + Bv + Cv^2) & v_{cri} \leq v < v_r \\ P & v_r \leq v < v_{co} \\ 0 & v > v_{co} \end{cases} \quad (15)$$

In (15), A , B , and C depends on WTG parameters and v_{cri} , v_r , v_{co} is starting speed, nominal speed and maximum speed of WTG, respectively, that is illustrated in Fig. 3.

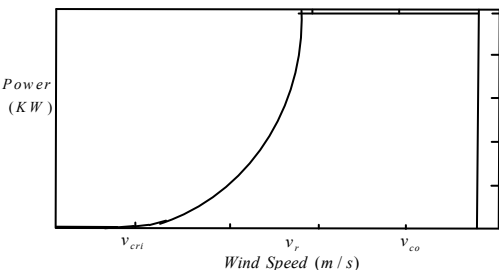


Fig. 3. The output voltage of a WTG

4. Power System Controlling Methods

The two proposed control methods based on average maximum transfer power and minimum power factor correction are considered for controlling UPFC-MC which is installed on power system including WTGF. These two methods are described in [13] for UPFC-MC which is used on a sample power system with unbalanced loads. In average maximum transfer power that its controlling part is illustrated in Fig. 4(a), the average active and reactive powers are determined from instantaneous active and reactive powers through injected voltages and currents on each three phases, and after that, compared with reference values of active power, P_{ref} , and reactive power, Q_{ref} , then, through this power flows are controlled and regulated. As it mentioned, the power system had different loads on each three phase, so, their phase power factors were different. In minimum power factor correction method that is illustrated in Fig. 4(b), the aim of this controlling method is to set UPFC-MC controlling parameters in order to increase power factor of selected phase. As it can be seen in Fig. 4(b), in this method minimum power factor determined from injected voltages and currents. After that, the angle of obtained power factor was calculated and this angle transfer to controlling system and the UPFC-MC parameters were set through this way. The d-q-0 axis values are obtained by applying Park's transformation that applied to PI1 and PI2 controller. The value of I_q^* is set to zero in order to achieve unity power factor. Instantaneous angle values of three phase voltage can be obtained by using phase locked loop (PLL) block diagram.

5. Simulation Results

The studied power system is shown in Fig. 5 that UPFC-MC is illustrated between B_1 and B_2 buses. The conventional power plants are located at B_1 and B_3 buses. A three phase balanced load with $200MW$ value is connected to B_3 bus and a three phase unbalanced load with $(8000MW, 100MVar)$, $(5000MW, 100MVar)$, and $(10000MW, 100MVar)$ are connected to B_4 bus. Also, a WTGF is directly connected at B_4 bus where the load is the nearest to it and its type should be double-fed induction generator (DFIG). The maximum WTGF power is $20MVA$ that provided under different wind speed that is considered variable in this simulation. Other simulation parameters are presented with details in Table I.

Table 1. Power system parameters

Three-phase ac source 1	Rated voltage	$230kV \times 1.03$
	Frequency	$60Hz$
	Short circuit level	$8500MVA$
	Base voltage	$230kV$
	X_g / R_g	8
Three-phase ac source 2	Rated voltage	$230kV \times 1.03$
	Frequency	$60Hz$
	Short circuit level	$6500MVA$
	Base voltage	$230kV$
	X_g / R_g	8
Transmission lines	Resistance per unit length	$0.01273\Omega / km$
	Inductance per unit length	$0.9337mH / km$
	Capacitance per unit length	$12.74nF / km$
	Length 1	$100km$
	Length 2	$200km$
Shunt transformer	Nominal power	$150MVA$

	Frequency	$60Hz$
	Nominal voltage	$230kV / 25kV$
	Magnetization reactance and resistance	$500p.u.$
Series transformer	Rated voltage	$12.5kV / 15kV$
	Rated power	$150MVA$
	Magnetization reactance and resistance	$500p.u.$
IGBT switches	Internal resistance	0.001Ω
	Snubber resistance	$0.1M\Omega$
	Snubber capacitance	Infinite
WTGF	Nominal Power	$20MVA$
	Transformer	$200V / 230kV$
	Wind Speed	Variable

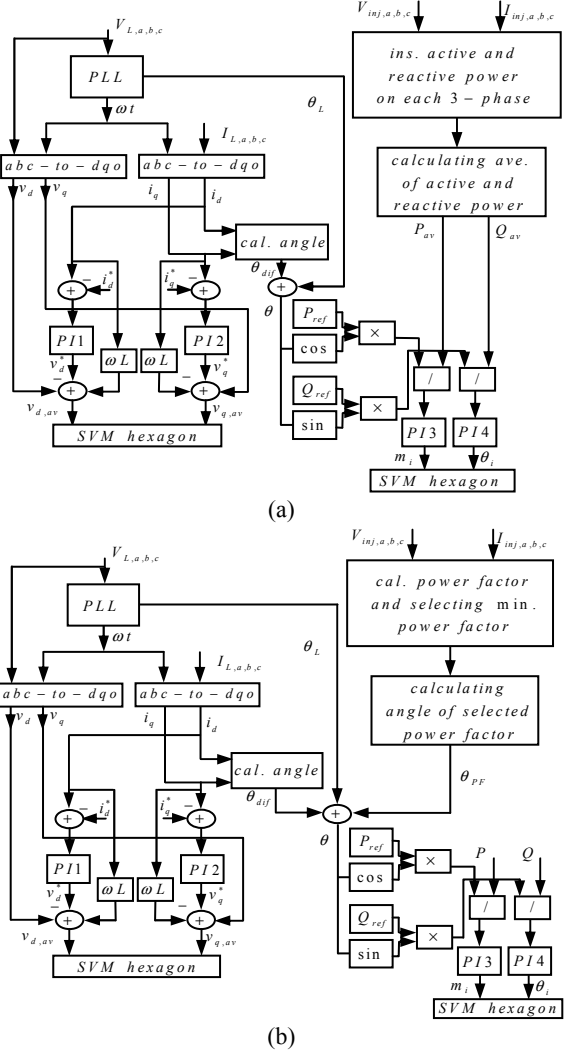


Fig. 4. Controlling methods of UPFC-MC; (a) maximum transfer power; (b) minimum power factor correction

During simulation, it was considered that $(10000MW, 100MVar)$ is controlled by circuit breaker (CB). By operating CB the three phase's loads are changing dynamical. The shunt side tried to reduce phase different between transmission lines voltage like to capacitance, and series side tried to control directly magnitude and angle of injected voltage when UPFC-MC is connected to power system. The voltage and current waveforms of phase "a" in shunt side for maximum power transfer and minimum power factor correction controlling methods are shown in Figs. 6 and 7, respectively. Also, the injected voltages of WTGF when power

system controlled by maximum power transfer and minimum power factor correction controlling methods are shown in Figs. 9(a) and (b), respectively. The injected voltage and current waveforms at bus B_2 are shown maximum power transfer and minimum power factor correction controlling methods in Figs. 9 and 10, respectively. According to Figs. 9 and 10, the difference between injected voltages and currents are small, in the other words, the power factor of injected value is near to unity. The active and reactive power flows in studied power system is illustrated in Fig. 11 with and without UPFC-MC under two controlling methods, WTGF connected, and dynamical loads. As it can be seen in this figure, the active and reactive power flows were increased and the transferred power on lines increased with UPFC-MC coordinate WTGF under two controlling methods considering loads that were changing dynamically through CB operating. As it is clear from Fig. 11(a) the active transferred powers was reached to $60MW$, $50MW$ and $47MW$ from $45MW$ values by applying maximum transfer power controlling method and WTGF, minimum power factor correction controlling method and WTGF, and only WTGF respectively, where the needed demand of active power was provided by WTGF when unbalanced loads were dynamically variable through CB operating. Also, the reactive power flow variation are shown in Fig. 11(b) that was increased to $1.2MVar$, $1.1MVar$ and $0.9MVar$ from $0.8MVar$ values by applying maximum transfer power controlling method and WTGF, minimum power factor correction controlling method and WTGF, and only WTGF, respectively.

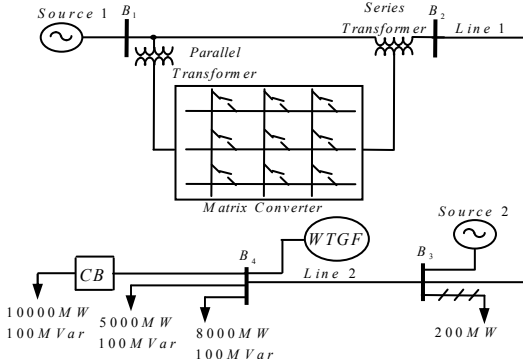


Fig. 5. Studied power system with UPFC-MC and WTGF

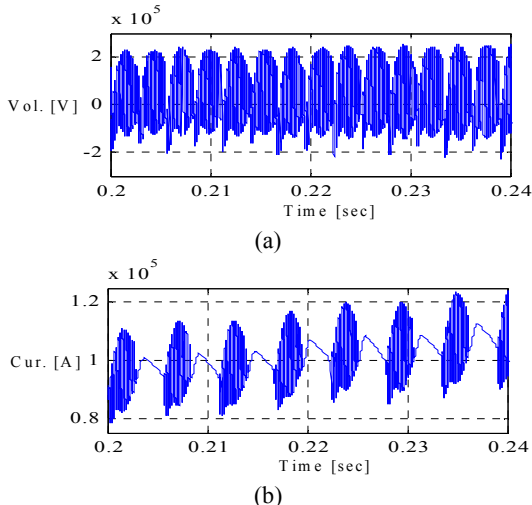


Fig. 6. Phase 'a' waveform of matrix converter by maximum transfer power control method; (a) voltage; (b) current

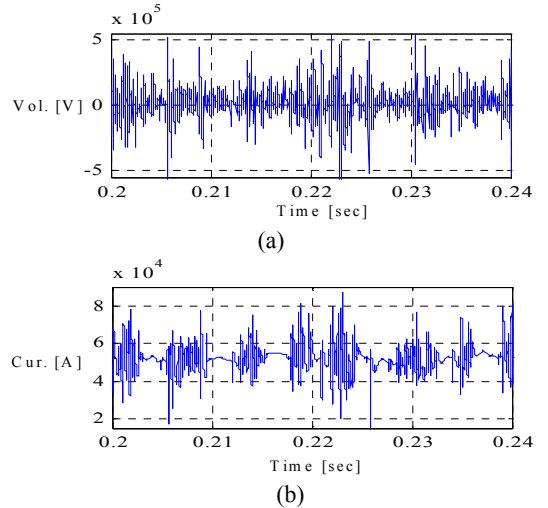


Fig. 7. Phase 'a' waveform of matrix converter by minimum power factor correction control method; (a) voltage; (b) current

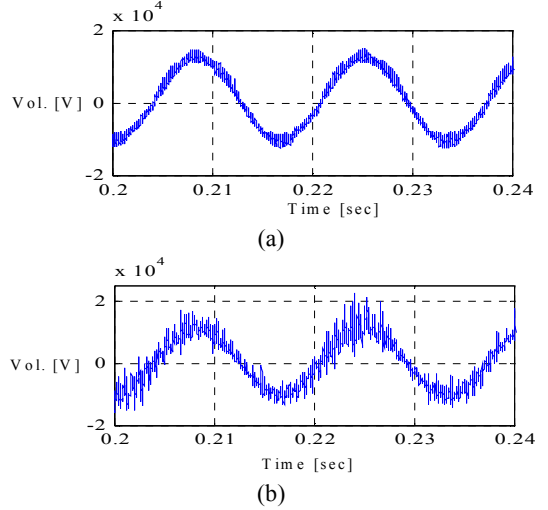


Fig. 8. Phase 'a' waveform of injected voltage of WTGF; (a) maximum transfer power control method; (b) minimum power factor correction control method

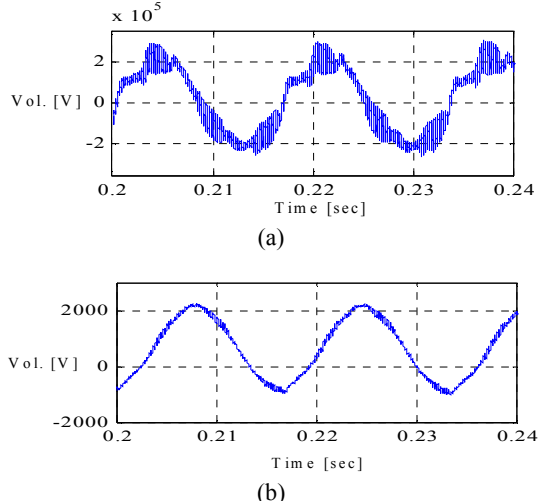


Fig. 9. Injected waveform of phase 'a' by maximum transfer power control method; (a) voltage; (b) current

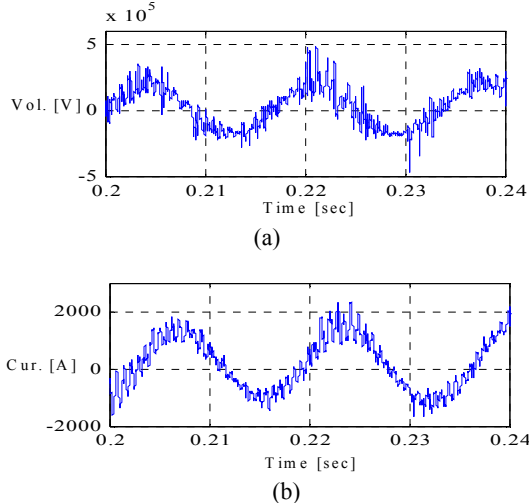


Fig. 10. Injected waveform of phase ‘a’ by minimum power factor correction control method; (a) voltage; (b) current

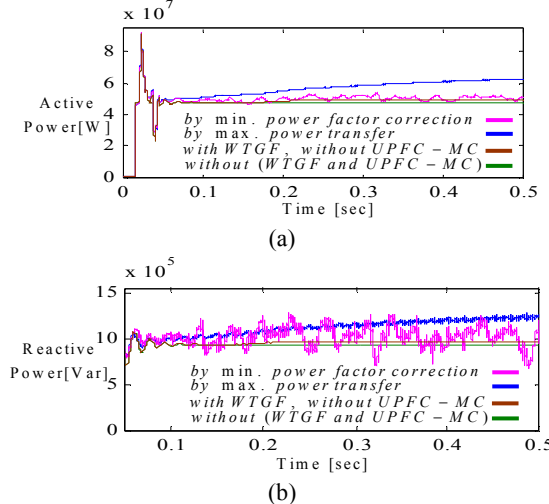


Fig. 11. Transmission line power flows, (a) real power, (b) reactive power

6. Conclusion

In this paper, a UPFC-MC and a WTGF are considered together for unbalanced loads under proposed controlling methods. Also, the different situations are considered for power system. According to simulation results, the needed power demand of studied power system provided by WTGF when unbalanced loads were changing and UPFC-MC can improve power flows on transmission lines. The simulation results shown that UPFC-MC can be operated with WTGF under proposed schemes and helped to WTGF for improving stability indices against dynamical loads variation.-MC and WTGF can operate coordinate and effect on reliability and protection level of power system, reducing the losses, and capacitance of power flows, positively.

7. References

- [1] F. M. Shahir and E. Babaei, “Dynamic Modeling of UPFC by Two Shunt Voltage-Source Converters and a Series Capacitor,” in *Proc. ICECT*, 2012, pp. 548-553.
- [2] F. M. Shahir and E. Babaei, “Evaluating of power system stability by UPFC via by Two Shunt Voltage-Source Converters and a Series Capacitor,” in *Proc. ICEE*, 2012.
- [3] N. G. Higorani and L. Gyugyi, *Understanding FACTS: concepts and technology of flexible ac transmission systems*, New Jersey: IEEE Press, 1999.
- [4] B. Geethalakshmi, G. Devanathan, and P. Dananjayan, “A novel structure of UPFC with matrix converter,” in *Proc. ICPS*, 2009, pp. 1-6.
- [5] A.R. Marami Iraaq, M. Tarafdar Haque, and E. Babaei, “A UPFC based on matrix converter,” in *Proc. PEDSTC*, pp. 95-100, 2010.
- [6] M. Hilal, M. Maaroufi, and M. Ouassaid, “Doubly fed induction generator wind turbine control for a maximum power extraction,” in *Proc. ICMCS*, pp. 1-7, 2011.
- [7] L. Barote, M. Georgescu, and C. Marinescu, “Smart storage solution for wind systems,” in *Proc. PowerTech*, pp. 1-6, 2009.
- [8] T. Karaipoom and I. Ngamroo, “Optimal superconducting coil integrated into DFIG wind turbine for fault ride through capability enhancement and output power fluctuation suppression,” *IEEE Trans. Sustainable Energy*, vol. 6, no.1, Dec. 2015.
- [9] M. F. M. Arani and Y. A-R. I. Mohamed, “Analysis and impacts of implementing droop control in DFIG-based wind turbines on microgrid/weak-grid stability,” *IEEE Trans. Power Systems*, vol. 30, no. 1, pp. 385-396, Dec. 2015.
- [10] Y. Tang, H. He, J. Wen, and J. Liu, “Power system stability control for a wind farm based on adaptive dynamic programming,” *IEEE Trans. Smart Grid*, vol. 6, no. 1, pp. 166-177, Dec. 2015.
- [11] W. Wei, F. Liu, S. Mei, and Y. Hou, “Robust energy and reserve dispatch under variable renewable generation,” *IEEE Trans. Smart Grid*, vol. 6, no. 1, pp. 369-380, Dec. 2015.
- [12] J. Monteiro, J. F. Silva, S. F. Pinto, and J. Palma, “Matrix converter-based unified power flow controllers: advanced direct power control method,” *IEEE Trans. Power Del.*, vol. 26, pp. 420-430, Jan. 2011.
- [13] F. M. Shahir, S. Ranjbar, and E. Babaei, “New Control Methods for Matrix Converter based UPFC under Unbalanced Load,” in *Proc. IICPE*, 2012, pp. 1-6.
- [14] F. M. Shahir and E. Babaei, “Evaluating the dynamic stability of power system Uusing UPFC based on indirect matrix converter,” in *Proc. ICECT*, 2012, pp. 554-558.
- [15] F. M. Shahir, E. Babaei, S. Ranjbar, and S. Torabzad, “Investigation of Power System Stability by Indirect Matrix Converter,” in *Proc. ICTPE*, 2013.
- [16] E. Babaei, S.H. Hosseini, G.B. Gharehpetian, and M. Sabahi, “A new switching strategy for 3-phase to 2-phase matrix converters,” in *Proc. SICE-ICASE*, 2006, pp. 3599-3604.
- [17] S. H. Hosseini and E. Babaei, “A new control algorithm for matrix converters under distorted and unbalanced conditions,” in *Proc. CCA*, 2003, pp. 1088-1093.
- [18] A. Alesina and M. Venturini, “Analysis and design of optimum amplitude nine-switch direct ac-ac converters,” *IEEE Trans. Power Electron.*, vol. 4, no. 1, pp. 101-112, August 1989.
- [19] L. Huber and D. Borovjevic, “Space vector modulated three phase to three phase matrix converter with input power factor correction,” *IEEE Trans. Ind. Appl.*, vol. 31, no. 6, pp. 1234-1246, Dec. 1995.